Characterization of high-overtone bulk acoustic resonators: applications to ultra-low noise microwave oscillators and miniature atomic clocks

R. Boudot[(1)], G. Martin[(1)], J-M. Friedt[(1)] and E. Rubiola[(1)]

[(1)]FEMTO-ST, CNRS, UBFC, ENSMM, 26 rue de l'épitaphe 25030 Besançon, France.
Email:rodolphe.boudot@femto-st.fr

INTRODUCTION

The generation of microwave signals with MEMS bulk acoustic wave (BAW) resonators is an exciting challenge. Such resonators allow the development of high-performance microwave sources combining low power consumption, small size, autonomy and ultra-low phase noise performances making them well-suited for applications such as radars, embedded electronics systems, telecommunications or embedded sensors.
In the family of MEMS acoustic resonators, high-overtone bulk acoustic (HBAR) resonators [1,2] are valuable candidates by demonstrating a possible direct operation frequency of a few GHz, state-of-the-art Qf products up to 10^{14} [3,4] and high-potential for wafer-level fabrication.
In this paper, we propose the description and characterization of AlN-sapphire HBAR resonators. Additional details are reported in [5]. Some detailed investigations are reported on a HBAR mode of interest at 2.3 GHz. We report the measurement of S-parameters, temperature coefficient of frequency, typical loaded Q-factor, sensitivity of the HBAR frequency to the input microwave power highlighting the existence of non-linear effects and residual phase noise measurements of the HBAR. The residual phase noise of the HBAR is found to increase with the input microwave power. A residual phase noise of -130 dBrad^2/Hz is measured at 1 Hz offset frequency at 2.3 GHz for low input microwave power (~6Bm). The HBAR resonator is inserted in a 2.3 GHz oscillator loop, allowing the demonstration of excellent phase noise performances at the level of -145 dBrad^2/Hz at 10 kHz offset frequency, in excellent agreement with the Leeson effect. In the last section of the manuscript, the HBAR-oscillator prototype (not integrated) is used as a local oscillator in a microcell-based coherent population trapping (CPT) Cs atomic clock laboratory-prototype. For this purpose, a low noise frequency doubling stage is implemented to up-convert the HBAR oscillator 2.3 GHz signal to 4.6 GHz (half of the Cs atom frequency). Fine tuning of the oscillator frequency to the atomic transition frequency is performed by adjusting of the HBAR temperature and implementation of a voltage-controlled phase shifter (VCPS) in the oscillator loop, preventing the use of a power-consuming direct digital synthesis (DDS). The HBAR-oscillator is successfully stabilized to the atomic transition, allowing to demonstrate when locked to the atoms, a preliminary clock short-term fractional frequency stability at the level of 7 10^{-11} $\tau^{-1/2}$ up to about 10 s, limited by the detected atomic resonance signal to noise ratio.

DESCRIPTION AND CHARACTERIZATION OF THE HBAR RESONATOR

Figure 1 shows the architecture of the HBAR resonator, designed by CEA-LETI, Grenoble, France.

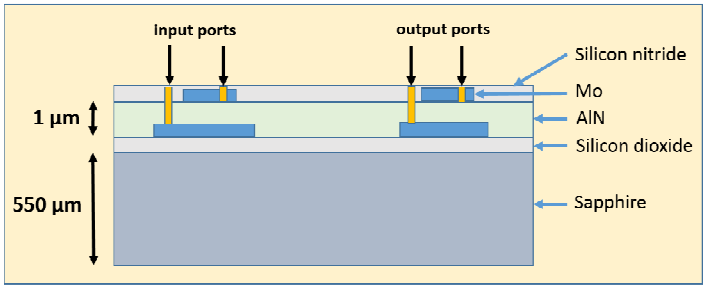

Figure 1: Architecture of the AlN-Sapphire HBAR resonator.

It consists of a substrate made of sapphire with a thickness of 550 µm, a width of 1700 µm and a length of 875 µm. On this substrate is found a piezoelectric film made of AlN material with a thickness of 1 µm. This resonator is a dual-port resonator and allows to operate in the transmission mode [6]. The idea is to ensure the coupling of acoustic waves between two adjacent resonators, achieved by implementing two resonators close to one another, allowing for evanescent waves between the resonator electrodes to overlap. The HBAR is connected through SMA connectors and the ensemble is implemented in a small duralumin packaging box (see figure 2). A thermistance and heating resistance are implemented in order to ensure the thermal control of the resonator at the mK level.

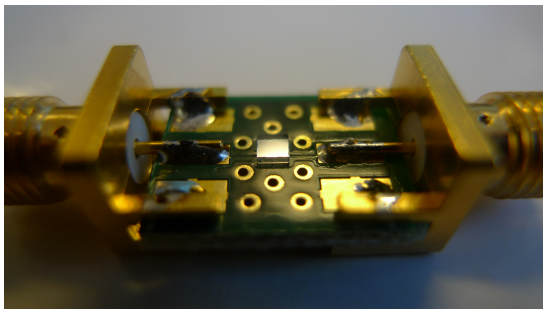

Figure 2: Photograph of the HBAR resonator.

Figure 3 reports the S_{21} parameter (magnitude and phase) of the HBAR resonator mode at about 2.3 GHz. The HBAR exhibits two well-visible eigenmodes, explained by the dual-port structure of the HBAR resonator. Losses of the resonator are about 16 dB at resonance.

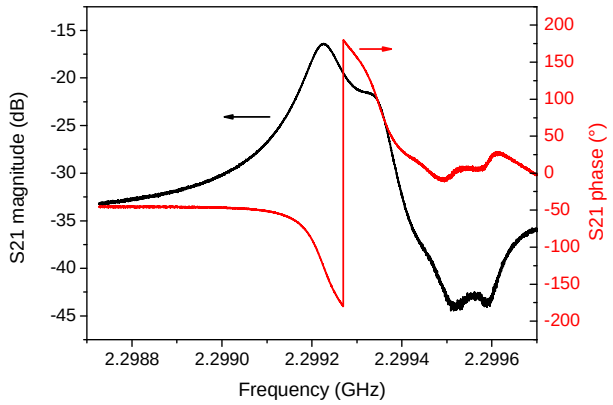

Figure 3: S_{21} parameter (magnitude and phase) of the HBAR resonator mode at about 2.3 GHz.

Figure 4 reports the HBAR mode frequency and loaded Q-factor Q_L versus the HBAR temperature. The HBAR temperature coefficient of frequency (TCF) is measured to be -24.7 ppm/K. While such a TCF appears large and might prevent high stability oscillator operation, we will actually benefit from this high sensitivity by tuning the oscillator frequency to an atomic transition by selecting the HBAR temperature: the HBAR mode spacing of 10 MHz, determined by the low acoustic loss sapphire substrate thickness, is swept around 2.3 GHz by tuning the temperature in a 180 K range. The loaded Q-factor is in the range of 28 000 and found to increase slightly with temperature between 40 and 90°C.

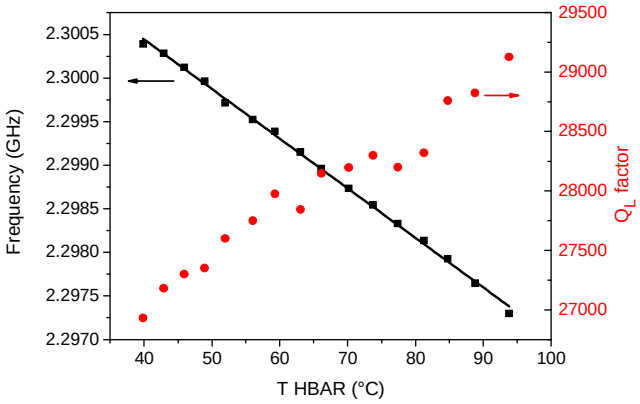

Figure 4: Frequency and Q_L factor of the HBAR versus the temperature.

Figure 5 shows the evolution of the HBAR frequency versus the microwave input power. Experimental data are correctly fitted by a linear function with a slope of -1350 Hz/mW (-5.9 10^{-10}/µW in fractional value). These values are

close to typical amplitude-frequency coefficient values, of few 10^{-10} to 10^{-9} / µW for quartz resonators [7]. As detailed in [5], we think that the HBAR frequency variation is here caused by non-linear effects and not by power-induced thermal heating of the HBAR resonator. Indeed, with increased input microwave power incident on the HBAR input port, we observed a clear and significant distortion of the resonance curve away from the Lorentzian line shape. In this experiment, the resonance shape was found to be slightly analogous to lineshapes induced by spring-softening Duffing non-linearity phenomena [8] frequently observed in MEMS or NEMS resonators.

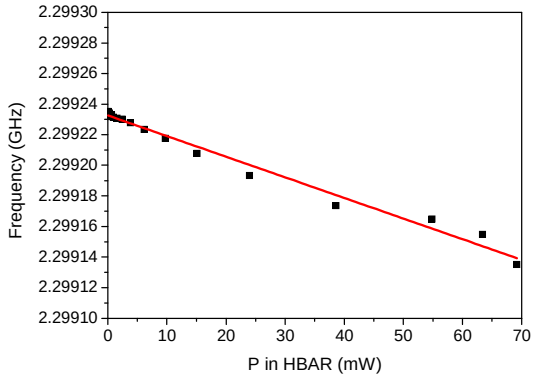

Figure 5: Frequency of the HBAR resonance versus the input port microwave power.

We measured the residual phase noise of the HBAR resonator. The setup description is the following. A 2.3 GHz source (Keysight E8257D) is power-split into two arms. The first arm involves a microwave amplifier and the HBAR resonator. The second arm only contains a microwave phase shifter to adjust the quadrature condition between arms of the phase noise measurement system. Both arms are directed to a microwave mixer operating as a phase detector. The output of the mixer is low pass-filtered, dc amplified and sent to a FFT analyzer. In this single-resonator bridge configuration, an issue is that the frequency fluctuations of the source can be converted into phase fluctuations through the resonator-based frequency-phase converter. The higher the Q factor, the higher the contribution of the source noise to the overall output noise. Figure 6 reports the residual phase noise of the HBAR resonator for several input microwave power values. The contribution of the source is shown in grey and is shown to be the main limitation of the measurement for f > 2 kHz. The noise of the mixer-based setup is shown in black and is at the level of -140 dBrad^2/Hz at 10 Hz offset frequency. The HBAR residual phase noise is clearly visible for 10 Hz < f < 1 kHz and is found to increase with increased input power. It is found at the level of -120 dBrad^2/Hz at 1 Hz offset frequency for an input power of 9.5 dBm.

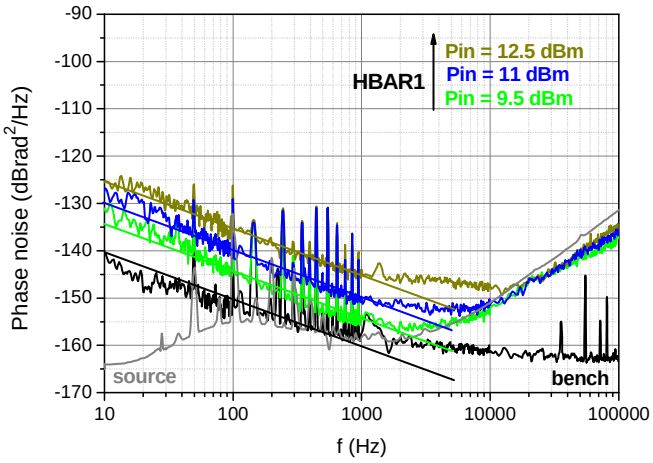

Figure 6: Residual phase noise of the HBAR resonator for various values of the incident microwave power.

For an input power of 6.5 dBm, we measured a phase noise of -130 dBrad^2/Hz at f = 1Hz. In the presence of flicker, the Allan deviation σ_{yq} (τ), stability of the resonator frequency, i.e., the time-domain stability of an oscillator in which the resonator is the only source of frequency instability, is given from:

$$\sigma_{yq}^2(\tau) = \frac{2\ln(2)}{4Q_L^2} b_{-1}$$

with b_{-1} the flicker phase noise value at f = 1Hz. From our experimental phase noise data, with b_{-1} = -130 dBrad^2/Hz, we estimate that the Allan deviation σ_{yq} (τ = 1 s) is about 6.7 10^{-12}.

DEVELOPMENT OF A HBAR-BASED LOW PHASE NOISE OSCILLATOR

We have developed a low phase noise 2.3 GHz oscillator based on the HBAR resonator. Figure 7 shows the architecture of the oscillator. The HBAR resonator is associated in a feedback loop with two sustaining amplifiers of total gain ~ 25 dB, a microwave isolator, a band pass filter and a phase shifter to satisfy Barkhausen conditions. The HBAR resonator can be finely temperature controlled. Moreover, a voltage-controlled phase shifter is implemented in the feedback loop. On the one hand, it is used for fine tuning of the oscillator output frequency (DC bias). On the other hand, it allows to create modulation sidebands needed for locking the oscillator on the atomic transition frequency.

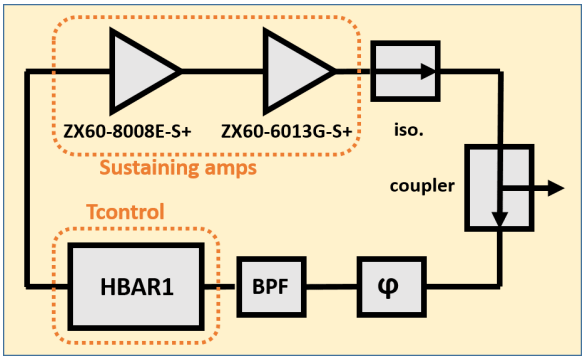

Figure 7: Architecture of the HBAR-based 2.3 GHz oscillator

Figure 8 shows the absolute phase noise of the HBAR-oscillator at 2.3 GHz The phase noise of the sustaining amplifier is reported for information. The phase noise floor of the oscillator is in good agreement with the phase noise floor of the amplifier [9], in excellent agreement with the amplifier thermal noise FkT/Pin where F is the amplifier noise figure, kT the thermal energy and Pin the amplifier input power (-13 dBm). The output oscillator signal phase noise is in excellent agreement with the Leeson effect [10] with a f^{-3} slope for 5 Hz < f < 1 kHz, a f^{-2} slope for 1kHz < f < 40 kHz (with $\upsilon_0/(2Q_L)$ = 40 kHz the Leeson frequency, the resonator bandwidth). The HBAR-based oscillator exhibits excellent phase noise performances at the level of -145 dBrad^2/Hz at 10 kHz. Phase noise performances of the HBAR oscillator are better than those of a state-of-the-art 100 MHz OCXO ideally frequency-multiplied to 2.3 GHz [11]. They are also significantly better than those of a conventional local oscillator [12] used in miniature atomic clocks (MACs) (see figure 8).

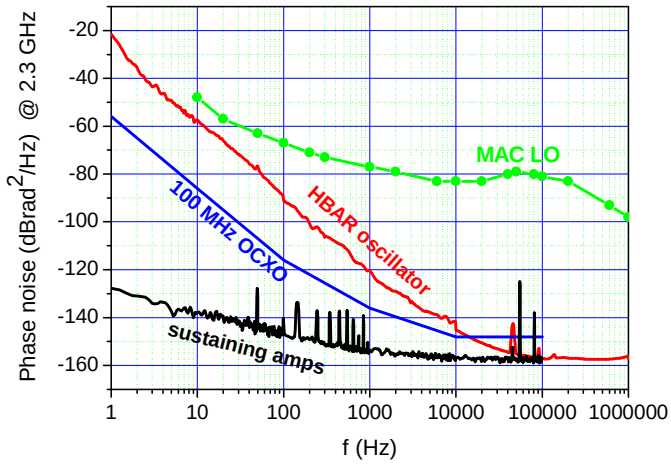

Figure 8: Phase noise of the sustaining amplifier and HBAR-based oscillator at 2.3 GHz. The latter is compared with the absolute phase noise of a state-of-the-art 100 MHz OCXO ideally frequency-multiplied to 2.3 GHz. Also, the phase noise at 2.3 GHz of a conventional MAC LO [12] is reported for comparison.

APPLICATIONS TO A MICROCELL-BASED ATOMIC CLOCK

The physical phenomenon of coherent population trapping (CPT) [13], combined with the progress of MEMS technologies and semi-conductor lasers, has allowed over the last decade the development of miniature atomic clocks (MACs) [14] with a typical volume of 15 cm^3, a power consumption of 150 mW and a fractional frequency stability of 10^{-11} at 1 day integration time.

Local oscillators for Cs MAC applications must satisfy many stringent requirements. They should have an output frequency of 4.596 GHz (half-frequency of the Cs atom at 9.192 631 770 GHz) to be resonant with the alkali atom, a tunable output power of -10 to 0 dBm to drive the VCSEL laser, modulation capabilities (frequency modulation and modulation depth up to a few kHz), a frequency resolution at 1-10 mHz level not to limit the clock frequency stability, a phase noise lower than -80 dBc/Hz at f = 1 kHz not to degrade the clock short-term frequency stability at the level of 10^{-11} at 1 s through the so-called intermodulation effect [15] and a free-running Allan deviation lower than 10^{-7} at 1 s.

To date, the local oscillator in a Cs MAC consists in general of a 4.596 GHz voltage-controlled oscillator (VCO) phase-locked to a 10 MHz quartz oscillator through a fractional-phase locked loop. Different designs were proposed in the literature [12,14]. Nevertheless, it has to be noted that today, the LO and associated frequency synthesis chain electronics represent more than 50% of the total power budget of a miniature atomic clock. Phase noise performances of these architectures are modest but remain to date sufficient. For information, Figure 8 compares the phase noise of a 2.3 GHz signal ideally-generated from a classical 10 MHz MAC LO to our 2.3 GHz HBAR-oscillator. In that sense, we proposed in an investigation experiment the use of the above-described HBAR-oscillator as a local oscillator of a microcell-based Cs vapour cell atomic clock based on coherent population trapping (CPT).

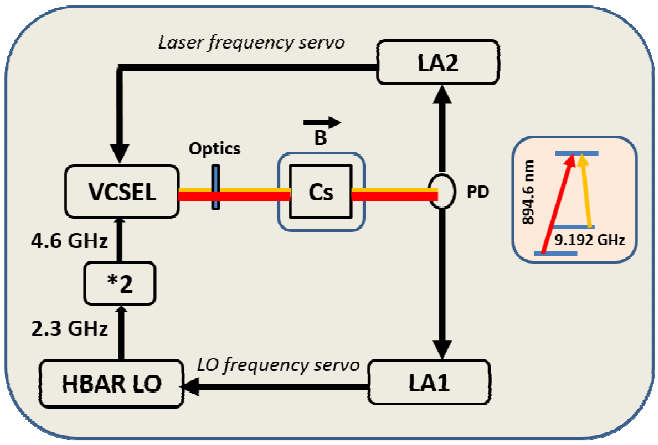

Figure 9: Principle of the CPT atomic clock. The HBAR LO 2.3 GHz signal is frequency doubled to 4.596 GHz. This signal drives a VCSEL laser which generates a bi-chromatic optical field at 895 nm. The laser beam is shaped, circularly polarized and sent into a Cs vapor micro-fabricated cell filled with Ne buffer gas. When the frequency difference between both optical lines is exactly equal to 9.192 GHz, atoms are pumped in a so-called dark state which increases the light transmission through the cell. The CPT resonance is detected by a photodiode. The output signal of the photodiode is sent into two lockin amplifiers (LA). LA1 is used for laser frequency stabilization by synchronously modulating-demodulating the laser dc current (laser frequency). LA2 is used for the HBAR LO frequency by synchronously modulating-demodulating the VCPS in the HBAR oscillator. The output 4.6 GHz at the output of the doubler is extracted with a coupler (not shown on the figure) and compared to the 4.6 GHz signal from a high-performance commercial microwave synthesizer driven by a hydrogen maser for frequency stability measurement. The inset on the fight of the figure shows the energy diagram involved in the CPT phenomenon.

Figure 9 presents the Cs CPT clock experimental setup. The laser source is a 25 MHz-linewidth custom-designed VCSEL tuned at 894.6 nm on the Cs D_1 line, designed by Ulm University [17]. The laser injection current is directly modulated at 4.596 GHz by the HBAR-based local oscillator (frequency-multiplied by 2) to generate two phase-coherent first-order optical sidebands frequency-split by 9.192 GHz for CPT interaction. The output laser beam, circularly polarized, is sent into a micro-fabricated Cs vapor cell [18] filled with a pressure of Ne buffer gas (113 Torr at 80°C). The input power is 30 µW. The microcell temperature is stabilized to within 1mK around 84°C. The laser power transmitted through the cell is detected by a photodiode. The output signal is used both for laser frequency stabilization and local oscillator frequency stabilization.

The 2.3 GHz output signal of the HBAR-oscillator is frequency-doubled to 4.596 GHz with a frequency doubler (Minicircuits ZX90-2-36S). The 4.596 GHz signal is bandpass-filtered with a 50-MHz bandwidth filter and amplified to a power up to 10 dBm with an amplifier (Minicircuits ZX60-8000ES+). A variable attenuator is used at the output to adjust if required the microwave power that drives the VCSEL laser. The tuning of the LO output frequency to the

atomic line is performed in two steps. A first coarse tuning of the LO frequency is done by adjusting the HBAR temperature. Once around the Cs resonance, a fine tuning of the LO frequency is performed by tuning finely the bias voltage of the VCPS. The tuning voltage-frequency sensitivity was measured to be about 8 kHz/V around the chosen set-point.
We succeeded to stabilize the HBAR-oscillator frequency to the atomic transition frequency. This was achieved without the use of any additional direct digital synthesis (DDS) and only with fine tuning of the VCPS. For measurement of the 4.596 GHz LO frequency stability, a comparison is performed with the 4.6 GHz signal from a commercial synthesizer driven by a hydrogen maser.
Figure 10 reports the Allan deviation of the HBAR-oscillator in free-running (HBAR temperature stabilized) and locked regimes. The stabilization to the atom frequency allows to improve the short-term fractional stability of the LO from 2 10^{-9} to 7 10^{-11} at 1 s integration time [19]. At 1000 s integration time, the stability of the HBAR LO is improved by about three orders of magnitude compared to the free-running regime.

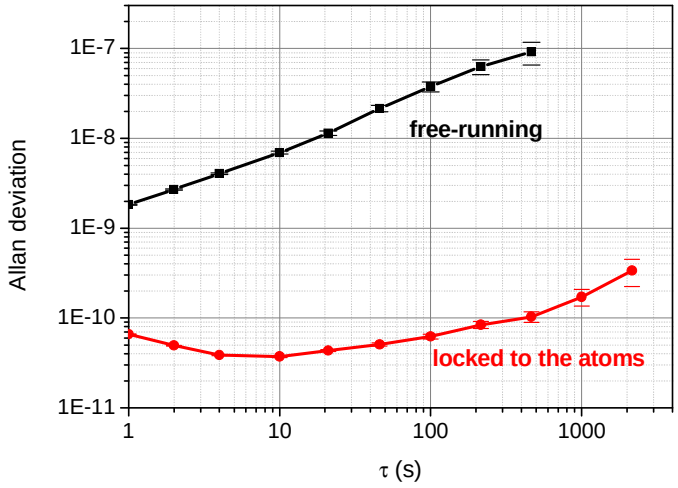

Figure 10: Allan deviation of the HBAR oscillator in free-running and locked regime (to the atoms).

DISCUSSIONS

HBARs exhibit several drawbacks. First, an inherent characteristic of HBARs is their multi-mode spectrum (due to materials superposition) that complicates their use in an oscillator and forces one to filter the response to select a single resonance. A second issue is the initial difficulty to tune finely the output frequency of the HBAR resonator due to the difficulty to control accurately thicknesses of materials during the fabrication process. Moreover, the HBAR we used here presents a quite high temperature sensitivity of about -24 ppm/K. Techniques exist to reduce the HBARs TCF but often at the expense of a degradation of the Q-factor and additional technological steps during the resonator fabrication.
In this study, after detailed characterization of the HBAR, we tried to convert these drawbacks into advantages to use the HBAR as a local oscillator in a microcell atomic clock application. Our strategy was to use both the HBAR temperature sensitivity and the exploitation of a VCPS in the oscillator loop to tune finely and stabilize successfully the oscillator output frequency to the atomic transition frequency. The VCPS allowed a frequency response of 8 kHz/V. A resolution of 1 µV would then allow a frequency resolution of 8 mHz, which is satisfying for MAC applications.
No special integration and packaging efforts were done in this work. Nevertheless, related activities in the literature demonstrate that such HBAR-LO architectures are compatible with integration at the chip level and low power consumption requirements for MAC applications. Ideally, for a MAC application, the temperature setpoint of the HBAR should be fixed at about 90°C to support MACs typical operation temperature ranges.
Other potential obstacles exist. In standard MACs, the output useful signal frequency is 10 MHz. In a potential HBAR-based oscillator Cs vapor cell MAC, the LO is frequency-stabilized at 4.596 GHz. This microwave frequency is not well-adapted for standard widespread applications. This issue would impose certainly to use a frequency divider to down-convert the 4.596 GHz signal to about 100 or 10 MHz, adding certainly 10-20 mW on the total power consumption of the system. Moreover, in the architecture presented here, modulation of the VCPS at about 1 kHz for tuning and stabilization of the oscillator to the atomic frequency could appear as an undesired spurious signal on the useful signal to be filtered or rejected for correct exploitation. At the end, we note that the combination of a HBAR-LO with stabilization to the atoms could be an interesting solution to propose an extremely small and low power consumption source demonstrating excellent spectral purity (intrinsic phase noise of the LO) and excellent long-term stability (thanks to the atoms).

CONCLUSIONS

We reported the detailed characterization of a 2.3 GHz AlN-Sapphire high-overtone bulk acoustic resonator (HBAR), with loaded Q-factor of about 28000 and insertion losses of 15–20 dB. The temperature coefficient of frequency of the HBAR is about -25 ppm/K. The power-induced fractional frequency variation of the HBAR resonance is measured to be about -6 10^{-10}/μW. The residual phase noise of a HBAR is measured in the range of -110 to -130 dBrad^2/Hz at 1 Hz Fourier frequency. This yields an ultimate HBAR-limited oscillator Allan deviation about 6.7 10^{-12} at 1 s integration time. The 1/f noise of the HBAR resonator is found to increase with the input microwave power. The HBAR resonator was used for the development of a low phase noise 2.3 GHz oscillator with a phase noise of -145 dBrad^2/Hz at 10 kHz offset frequency, in excellent agreement with the Leeson effect. The HBAR LO, with the help of a frequency doubling stage to reach 4.596 GHz, was used successfully as a local oscillator in a CPT-based Cs microcell atomic clock, demonstrating a fractional frequency stability of 7 10^{-11} at 1 s integration time.

ACKNOWLEDGMENTS

The authors thank C. Rocher and P. Abbé (FEMTO-ST) for help with electronics stuff, the MOEMS Group of FEMTO-ST (in particular C. Gorecki, V. Maurice, N. Passilly, J. Rutkowski and S. Bargiel) for the Cs microcell fabrication used in this study. The authors would like to thank Vincent Giordano (FEMTO-ST) for fruitful discussions on resonator nonlinearities and phase noise measurements. The authors acknowledge David Rabus and Sébastien Alzuaga (FEMTO-ST) for HBAR TCF calculations. The authors thank A. Reinhardt and P. P. Lassagne (CEA-LETI) for supplying us the HBAR resonators.
This work has been partly supported by the Agence Nationale de la Recherche (ANR) Project Equipex Oscillator IMP. The Oscillator IMP Project funded in the frame of the French national Projets d'Investivement d'Avenir (PIA) targets at being a facility dedicated to the measurement of noise and short-term stability of oscillators and devices in the whole radio spectrum (from MHz to THz), including microwave photonics. This work has been also partly supported by LabeX FIRST-TF, Direction Générale de l'Armement (DGA) and Région de Franche-Comté.

REFERENCES

[1] K. M. Lakin, G. R. Kline and T. McCarron, IEEE Trans. Microwave Theory Tech., vol. 41, 2139, 1993.
[2] K. M. Lakin, IEEE Trans. Ultrason. Ferroelec. Freq. Contr., vol. 52, 707, 2005.
[3] D. S. Bailey, M. M. Driscoll, R. Jelen and B. R. McAvoy, IEEE Trans. Ultrason. Ferroelec. Freq. Contr., vol. 39, 780, 1992.
[4] M. M. Driscoll, R. A. Jelen and N. Matthews, IEEE Trans. Ultrason. Ferroelec. Freq. Contr., vol. 39, 6, 774, 1992.
[5] R. Boudot, G. Martin, J. M. Friedt and E. Rubiola, Journ. Appl. Phys. 120, 224903 (2016).
[6] A. Reinhardt, M. Delaye, J. Abergel, V. Kovacova, M. Allain, L. Andreutti, D. Mercier, J. Georges, F. Tomaso and P. Lassagne, Proc. IEEE International Ultrasonics symposium (IUS), (IEEE2013), pp. 1922-1925.
[7] E. Rubiola, J. Groslambert, M. Brunet and V. Giordano, IEEE Trans. Ultrason. Ferroelec. Freq. Contr., vol. 47, 2, 361-368 (2000).
[8] A. H. Nayfeh and D. T. Mook, Nonlinear oscillations (Wiley, 1995), figure 1.5, p 9.
[9] R. Boudot and E. Rubiola, IEEE Trans. Ultrason. Ferroelec. Freq. Contr., vol. 59, 12, 2613, 2012.
[10] D. B. Leeson, Proc. IEEE 54, 2, 329 (1966).
[11] B. François, C. E. Calosso, M. Abdel Hafiz, S. Micalizio and R. Boudot, Rev. Sci. Instr. 86, 094707 (2015).
[12] R. Lutwak et al., The chip-scale atomic clock – prototype evaluation, 39th Precise Time and Time Interval meeting pp 269-290, (2007).
[13] G. Alzetta, A. Gozzini, L. Moi, and G. Orriols, Il Nuovo Cimento B Ser. 36, 5 (1976).
[14] S. Knappe, in Comprehensive Microsystems, edited by Y. B. Gianchandani (Elsevier B, Amsterdam, 2007), Vol. 3, pp. 571–612.
[15] C. Audoin, V. Candelier, and N. Dimarcq, IEEE Trans. Instrum. Meas. 40, 121 (1991).
[16] Y. Zhao, S. Tanner, A. Casagrande, C. Affolderbach, L. Schneller, G. Mileti, and P. A. Farine, IEEE Trans. Instrum. Meas. 64, 263 (2015).
[17] F. Gruet, A. Al Samaneh, E. Kroemer, L. Bimboes, D. Miletic, C. Affolderbach, D. Wahl, R. Boudot, G. Mileti and R. Michalzik, Optics Express 21, 5, 5781 (2013).
[18] M. Hasegawa, R. Chutani, C. Gorecki, R. Boudot, P. Dziuban, V. Giordano, S. Clatot, and L. Mauri, Sens. Actuators, A 167, 594 (2011).
[19] T. Daugey, J. M. Friedt, G. Martin and R. Boudot, Rev. Sci. Instr. 86, 114703 (2015).